PROCEEDINGS
SPIE—The International Society for Optical Engineering

Fullerenes and Photonics III

Zakya H. Kafafi
Chair/Editor

5–6 August 1996
Denver, Colorado

Sponsored and Published by
SPIE—The International Society for Optical Engineering

Volume 2854

From Astrophysics to Mesoscopic Physics – A Sightseeing Tour in the World of Clusters and Fullerenes

A. Rosén[1], D. Östling[1], P. Apell[2] and D. Tomanek[1,3]

[1]Department of Physics, Göteborg University and
Chalmers University of Technology, S-412 96 Göteborg, Sweden.
[2]Department of Applied Physics, Chalmers University of Technology and
Göteborg University, S-412 96 Göteborg, Sweden.
[3]Department of Physics and Astronomy, Michigan State University,
East Lansing, Michigan 48824 -1116, USA

ABSTRACT

The discovery of the fullerenes in 1985 by Kroto, Heath, O'Brien, Curl and Smalley and the development of a method for production of macroscopic amounts in 1990 by Krätschmer, Lamb, Fostiropoulos and Huffman opened a new area of carbon research with possible production of new materials with unique properties. The field has developed further later on with discoveries of nanotubes, metal filled nanotubes, carbon onions and more recently metal covered fullerenes. All these new discoveries show how cluster science opens approaches to the area of meososcopic physics. The general trend is here in the direction from small to large contrary to the general trend of modern mesoscopic physics or micro-electronics where the movement is from large to small. It is especially fascinating how the whole area of fullerene research was initiated by problems in astrophysics. Originally Krätschmer and Huffman had the intention to explain an observed strong extinction from interstellar dust and produced in experiments special carbon soot with a characteristic optical absorption known as *"the camel hump smoke"*. This paper gives a short overview of some of our more recent theoretical work of the electronic properties of C_{60}, metal covered C_{60} and nanotubes. In addition some results are also presented of optical properties of metal covered C_{60} as a function of metal coverage.

1 INTRODUCTION

Research on clusters during the past twenty years [1-4] has generated a new interdisciplinary field in which knowledge from many disciplines as nuclear, atomic, molecular, astro and solid state physics has been very valuable for the present status of this field. Today, free and deposited clusters, ranging from a few atoms to a few thousand of atoms can be produced for many elements in the periodic table. These clusters have also in many cases been characterized with respect to different electronic properties and in a few cases geometrical structure using experimental methods developed in studies of atoms, small molecules or solids. The knowledge obtained from such studies, as for example the experimental discovery of the icosahedral packing in clusters of xenon in the group of Recknagel in 1981 [5], initiated a new direction in the earlier established field of small particles. Probably even more exciting was the discovery of magic numbers for clusters of alkali elements in the group of Knight in 1984 [6]. Their discovery verified a shortly earlier prediction by Ekardt [7] of the existence of

SPIE Vol. 2854 • 0-8194-2242-8/96/$6.00

electronic shell structure for the delocalized electrons in clusters of alkali elements. The further development of the so-called self-consistent jellium model [3,4,8] for treatment of systems with a large number of fermions have resulted in many exciting discoveries as magic numbers, super shells [9,10] and clusters characterized as shells of atoms [11] in which one explores the unknown area by moving in the direction from small to large units i.e. between atomic/molecular physics and solid state physics. This kind of exploration is opposed to the trends in modern mesoscopic physics, micro-electronics, nano-technology or materials science [12,13], where the general direction today is a movement from large to small.

Before 1985 carbon was known to exist in two structures, graphite with the sp^2 bonding and diamond with sp^3 bonding which had quite different material properties. The whole field of carbon research has, however, changed totally after the discovery of fullerenes as C_{60} by Kroto, Heath, O'Brien, Curl and Smalley in 1985 [14] using the laser vaporization method and, in particular, after Krätschmer, Lamb, Fostiropoulos and Huffman [15,16] using the electric arc evaporation method. The research by in particular Kroto, Krätschmer and Huffman [17-20] were mainly motivated from problems in astrophysics aiming at producing particles of carbon for explanation of an observed strong extinction from interstellar dust [21]. The carbon soot they produced, having the characteristic optical absorption known as *"the camel hump smoke"* opened a whole new area of basic and applied carbon research [22-25]. An overview of the historical development of the field of fullerenes with special emphasis on the interplay between theoretical predictions of UV absorption [26], Raman and IR spectra [27] and the agreement with experimental data recorded more then four years before was discussed in an earlier SPIE proceedings [28].

The whole field of fullerene related species can be characterized as a number of serendipitous discoveries as the existence of of *"a whole zoo of fullerenes"* [29], *"endohedral ones"*[30] and later *"nanotubes of different diameters, lengths, number of shells which could be closed or open and filled with different types of materials"* [31-33] or *"Carbon onions"* [34]. Many of these discoveries represent a sightseeing tour in *"cluster science"* as visualized in Fig. 1 with the birth of a totally new area of materials science, mesoscopic physics or molecular eningeering which very few people could have imagined ten years ago. It is particluarly exciting that knowledge and research problems formulated to solve problems in astrophysics [35] has been so important for this development.

Today carbon compounds like C_{60} can function as templates for synthesising of new materials like the production of clusters of C_{60} [36], metal covered C_{60} [37-40] in the coevaporation of C_{60} with some metal for which the stability and the optical properties have been studied for some systems [41,42]. Another exciting area is the production of single and multiwalled nanotubes of controled sizes [43-46] for which the electronic behaviour depends on the chirality of the tube [47,48,25]. As example of other discoveries can be mentioned the recently found nanotubes [49] with values of Young modulus which are comparable with what is known for carbon fibres. The whole field of clusters and fullerenes represent such exciting areas of modern science where one can explore the presently unknown region between atomic/molecular physics, solid state physics which might have big impact on modern technology as materials science and mesoscopic physics.

Many of these clusters and fullerene based species are too big applying standard MO-LCAO methods for evaluation of the electronic structure and different properties. One has therefore in many cases developed simplified models which take into account the main physics and are comparatively easy to use. The previously mentioned jellium model [3,4,7,8] is such an example which has been used with great success in the evaluation of a number of properties for clusters of alkali and coinage elements. We present in this work a short summary of a recently developed numerical method [50] for evaluation of the electronic structure of single-wall and multi-wall nanotubes containing thousands of electrons. For analysis of special properties as the collective effects in atoms or solids models based on classical electrodynamic theory [51,52,53] has also been used with great success [54,55,56]. The C_{60} molecule is a strongly correlated system which implies that screening is important and must be included in the calculation of optical excitations. This can be achieved by inclusion of configuration interaction, as was done for example, in the CNDO/S-CI calculations [26,57]. A different approach, to account for the strong screening effects within the C_{60} molecule, is to evaluate the optical excitations using linear response theory based on, for example a type of tight-binding Hamiltonian as used by Bertsch *et al.* [58]. Recently a simplified Random Phase Approximation (RPA) has been introduced [59] as an extension of our earlier use of the sum-over-states approach [60,61,62]. This paper gives a short overview of some of our more recent works on the electronic structure, linear

optical properties of C_{60}, metal covered C_{60}, nanotubes and nanotubes filled with metals.

2 THEORY

2.1 Ground state calculations

Fig. 2 gives an overview of different presentations of C_{60}, which can form as a building block for production of new materials. Fig. 3 shows examples of metal covered C_{60} as exemplified with $M_{12}C_{60}$ and $M_{32}C_{60}$, where such systems has been observed for M = Li, Ca, Ba etc. [38-40]. Calculations for C_{60} can be done based on MO-LCAO methods while some approximate method is in general necessary for the bigger systems as for example C_{60} covered with a metal shell, long single and multi-wall nanotubes which can be empty or filled with some metal as will be outlined below. Furthermore, detailed calculations for such type of systems with many electrons will require computational methods which are highly accurate.

Using the standard MO-LCAO method [63,64] the molecular orbital wavefunctions ψ_i are constructed as

$$\psi_i(\vec{r}) = \sum_j \phi_j C_{ij} = \sum_j \sum_{\nu m} W^{jl}_{\nu m} u_{nl}(r_\nu) Y_{lm}(\hat{r}_\nu) C_{ij} \quad . \tag{1}$$

I.e. symmetry-adapted wavefunctions, ϕ_j, are projected from the atomic orbitals $u_{nl}Y_{lm}$ with coefficients $W^{jl}_{\nu m}$. The variational coefficients, C_{ij}, are obtained from the matrix secular equation,

$$(\mathrm{H} - \epsilon \mathrm{S})\,\mathrm{C} = 0 \quad , \tag{2}$$

where H and S are the Hamiltonian and overlap matrices, respectively. The Kohn-Sham Hamiltonian [65,66] enters in a one-particle equation of the Schrödinger form as

$$\left[-\frac{1}{2}\nabla^2 + v_{eff}(\mathrm{r})\right] \psi_i(\mathrm{r}) = \varepsilon_i\, \psi_i(\mathrm{r}) \quad , \tag{3}$$

where

$$v_{eff} = v_{bg} + v_e + v_{xc} \quad . \tag{4}$$

v_{bg} repesents the Coulomb potential from the nuclei or some background potential from the nuclei and core electrons. v_e is the Coulomb potential from the electrons and v_{xc} is the exchange-correlation potential for which we have used the Hedin-Lundqvist [67] form.

The atomic basis functions used for construction of the symmetry orbitals are obtained by solving the corresponding Kohn-Sham equations for the free atoms and ions. The matrix elements are evaluated using the numerical integration scheme developed by Boerrigter *et al.* [68]. The molecular charge distribution is fitted within the SCC approximation [69] or within the SCM approximation [70].

It is in principle possible to apply this technique for multi-walled nanotubes but the huge number of carbon atoms involved for describing an "infintiely" long nanotube (on the order of 10^3) makes a simplified approach more attractive. Our method has been to consider the 2s and 2p electrons of each carbon as active for formation

of orbitals and then to replace the individual point charges of the C^{4+} ions with a cylindrical two dimensional background having a uniform surface charge density σ. Using a C-C bond distance of 2.68 a.u. in a hexagonal lattice one obtains $\sigma = 0.428$ a.u.$^{-2}$. The potential from such a positive background charge of an infinitley long nanotube is then obtained by use of Gauss law [71] as

$$\begin{cases} v_{bg}(r) = -2\lambda \log(R) + C & r \leq R \\ v_{bg}(r) = -2\lambda \log(r) + C & r > R \end{cases} , \tag{5}$$

where λ is the the number of electrons per unit length $\lambda = 2\pi R\sigma$ and C is a constant. The total background potential for multi-walled nanotubes will be given as a superposition of this type of potentials with variuos radii R of the walls. A similar approach can also be used for infinitley long nanowires of a certain electron density for which the jellium potential for such a wire will be given as

$$\begin{cases} v_{bg}(r) = -\lambda((r/R)^2 - 1) - 2\lambda \log R + C & r \leq R \\ v_{bg}(r) = -2\lambda \log r + C & r > R \end{cases} , \tag{6}$$

where λ is the the number of electrons per unit length of the wire and C is a constant. The wavefunction and the corresponding radial equation will be given as [50]

$$\psi_{nmk}(r, \alpha, z) = \frac{1}{\sqrt{\pi L}} R_n(r) e^{im\alpha} \sin\left(\frac{k\pi}{L} z\right) ,$$

2.2 Random Phase Approximation

The Random Phase Approximation (RPA) has been successfully used for describing small-amplitude excitations in many-body systems and in particular for metal clusters as reviewed by Brack [4]. In the literature the RPA is presented in the framework of the Hartree-Fock (HF) theory [73]. We consider the RPA within the framework of DFT and the particle-hole excitations are created from the Kohn-Sham orbitals, as has recently been applied [74,75] for the analysis of optical properties of metal clusters. The RPA equation that determines the excitation energy spectrum $\hbar\omega_\lambda$ has the form [73]:

$$\begin{pmatrix} A & B \\ B^* & A^* \end{pmatrix} \begin{pmatrix} Y(\lambda) \\ Z(\lambda) \end{pmatrix} = \hbar\omega_\lambda \begin{pmatrix} Y(\lambda) \\ -Z(\lambda) \end{pmatrix} , \tag{8}$$

where

$$\begin{cases} A_{minj} &= \delta_{mn}\, \delta_{ij}\, (\varepsilon_m - \varepsilon_i) + V_{mjin} \\ B_{minj} &= V_{mnij} \end{cases} , \tag{9}$$

and the indices i, j (n, m) refer to hole (particle) states. If the one-electron orbitals are defined as Kohn-Sham orbitals the Coulomb interaction and exchange-correlation contribution lead to the following form of the particle-hole matrix element:

$$V_{mnij} = < mn|V_{\rm res}|ij > , \tag{10}$$

where [74]

$$V_{\rm res}(\mathbf{r} - \mathbf{r}') = \frac{1}{|\mathbf{r} - \mathbf{r}'|} + \frac{\delta v_{xc}[\rho]}{\delta\rho} \delta(\mathbf{r} - \mathbf{r}') . \tag{11}$$

Using the addition theorem

$$\frac{1}{|\mathbf{r} - \mathbf{r}'|} = 4\pi \sum_{l=0}^{\infty} \sum_{m=-l}^{l} \frac{1}{2l+1} \frac{r_<^l}{r_>^{l+1}} Y_{lm}^*(\theta', \phi') Y_{lm}(\theta, \phi) \tag{12}$$

and approximating a fullerene by an infinitely thin shell $r_< = r_> = R$ and also neglecting the exchange-correlation interaction, a matrix element $< mn|V_{res}|ij >$ may, considering dipolar oscillations along the z-axis, be approximated as

$$< mn|V_{res}|ij > \approx \lambda < m|z|i >< n|z|j > \quad , \tag{13}$$

where $z = r\cos\theta$ and $< m|z|i >$ and $< n|z|j >$ are the matrix elements for the dipolar transitions $m \rightarrow i$ and $n \rightarrow j$. $\lambda = R^{-3}$, where R is the radius of the infinitely thin shell. The forward and backward-going RPA amplitudes $Y(\lambda)$ and $Z(\lambda)$ obey the following orthonormalization condition:

$$\sum_{mi}(|Y_{mi}|^2 - |Z_{mi}|^2) = 1 \quad , \tag{14}$$

and the transition amplitude of a one-body operator $\hat{W}$ from the ground state to the λth excited state is given by

$$< \lambda|\hat{W}|0 >= \sum_{mi}[Y^*_{mi}(\lambda)W_{mi} + Z^*_{mi}(\lambda)W_{im}] \quad , \tag{15}$$

where $W_{mi} =< m|\hat{W}|i >$.

2.3 Classical Theory of a Coated Spherical Shell

When a system with an electronic ground state density ρ_0 is exposed to an external field V_{ext} an induced density ρ_{ind} results. From [51-53] we obtain the following classical equation of motion for ρ_{ind}:

$$\left\{\omega^2 - \omega_p^2(\mathbf{x})\right\}\rho_{ind}(\mathbf{x},\omega) = -\frac{1}{4\pi}\nabla\omega_p^2(\mathbf{x})\cdot\nabla V(\mathbf{x},\omega) \quad , \tag{16}$$

where $V(\mathbf{x},\omega) = V_{ext}(\mathbf{x},\omega) + V_{ind}(\mathbf{x},\omega)$, ω is the frequency of V_{ext} and V_{ind} is the potential from the induced charge density ρ_{ind} given by Poisson's equation $V_{ind} = \int d^3x'\rho_{ind}/|\mathbf{x}-\mathbf{x}'|$. $\omega_p^2(\mathbf{x}) \equiv 4\pi e^2\rho_0(\mathbf{x})/m$ and defines a local plasma frequency through the ground state electron density $\rho_0(\mathbf{x})$.

Assume that we have a metallic shell (C_{60}) with the constant electron density ρ_1 between the radii r_1 and r_2 and a metallic coating with the constant electron density ρ_2 between the radii r_2 and r_3, then the ground state and induced electron densities may be expressed as:

$$\rho_0(r) = \rho_{max}(\rho_1\,\theta(r-r_1)\,\theta(r_2-r) + \rho_2\,\theta(r-r_2)\,\theta(r_3-r)) \tag{17}$$

and

$$\rho_{ind}(r) = \sum_{l=0}^{\infty}\sum_{j=1}^{3} q_{jl}\,\delta(r-r_j)\,Y_{l0}(\theta) \quad . \tag{18}$$

Eq. (16) together with Eqs. (17–18) can be written in a compact matrix form as

$$\mathbf{A}\cdot\mathbf{Q} = \mathbf{R} \quad , \tag{19}$$

where

$$\mathbf{A} = \begin{pmatrix} \Omega^2 - \frac{l+1}{2l+1}\rho_1 & \frac{l}{2l+1}\rho_1\left(\frac{r_1}{r_2}\right)^{l-1} & \frac{l}{2l+1}\rho_1\left(\frac{r_1}{r_3}\right)^{l-1} \\ -\frac{l+1}{2l+1}(\rho_2-\rho_1)\left(\frac{r_1}{r_2}\right)^{l+2} & \Omega^2 - \frac{l}{2l+1}\rho_1 - \frac{l+1}{2l+1}\rho_2 & \frac{l}{2l+1}(\rho_2-\rho_1)\left(\frac{r_2}{r_3}\right)^{l-1} \\ \frac{l+1}{2l+1}\rho_2\left(\frac{r_1}{r_3}\right)^{l+2} & \frac{l+1}{2l+1}\rho_2\left(\frac{r_2}{r_3}\right)^{l+2} & \Omega^2 - \frac{l}{2l+1}\rho_2 \end{pmatrix} \quad . \tag{20}$$

$\mathbf{Q}$ is a vector representing the induced density, ρ_{ind}, with the three elements q_{jl}, and $\mathbf{R}$ is a vector describing an external driving field. If the external field is a simple dipolar one, for which $V_{ext} = -E_0\,r\cos\theta$, $\mathbf{R}$ has the components $R_{i1} = \sqrt{1/12\pi}\,E_0\,(\,\rho_{i+1} - \rho_i)$.

The matrix A contains the information on the excitation spectrum of the system so the three eigenvalues of A are the eigenmodes of the system. To obtain the photoabsorption cross section of the C_{60} molecule we evaluate the dipolar polarisability given by the expression

$$\alpha(\omega) = \int d^3x' \; z \, \frac{\rho_{ind}(x', \omega)}{E_0} \quad , \tag{21}$$

which gives the photoabsorption cross section through the formula

$$\sigma_{abs}(\omega) = \frac{2\pi e^2}{mc} \, \omega \, Im \, \alpha(\omega) \quad . \tag{22}$$

3 RESULTS AND DISCUSSION

3.1 Electronic structure and optical properties of C_{60}, $Na_{12}C_{60}$and $Na_{32}C_{60}$

We have earlier [59] analyzed the electronic structure of the bare C_{60}andC_{60} covered with 12 and 32 Li atoms. The calculations for the bare C_{60} were done using the bond lengths 1.458 Å for the pentagonal edge (single bonds) and the 1.401 Å for the bonds shared by hexagonal rings (or double bonds), as determined from gas phase electron diffraction [76]. The geometry for $Li_{12}C_{60}$ have been determined using the Car-Parinello method [77] as well as with a semi-empirical MNDO method [78] for the case when the Li atoms are located above the pentagonal phases. Both calculations give a change of the bond lengths within the cage compared with the experimental ones for the free C_{60} and also give values of the bond distances from the Li-atom to the cage corresponding to 1.54 Å and 1.77Å for the two calculations, respectively. In order to obtain some estimate of the bond distance of the Na atoms to the cage we have determined the bond distance by optimization the distance above a C_5H_5 ring with the result of 1.69 Å for Li which is between the values given above and 2.13 Å for Na. The optimized values determined in this way reflects mainly the approximate size of the atom and we have used this distance when Na is placed above a hexagonal ring in $Na_{32}C_{60}$. An energy level diagram for bare C_{60}, $Na_{12}C_{60}$ and $Na_{32}C_{60}$ is given in Fig. 4. We notice how the LUMO and LUMO + 1 levels of C_{60} are filled for $Na_{12}C_{60}$ while a number of new levels originating from the additional twenty Na atoms are occupied instead of filling the additional unoccupied C_{60} levels.

A further indication of the change of the electronic structure for metal covered C_{60} can be obtained by plotting the spherically averaged charge densities for the 60 π electrons of C_{60} and the last occupied 72 and 92 electrons for the metal covered C_{60} in Fig. 5. Comparison with the energy level diagram in Fig. 4 shows here more clearly how the first twelve valence electrons first go into the C_{60} levels and the additional valence electrons form a metal covered shell outside the cage. This is also in agreement with what is obtained in a Mulliken analysis of the molecular wavefunctions which shows a charge of about + 0.316 on each atom for the first 12 Na atoms which is further reduced to + 0.109 electrons on each atom for the 32 Na atom cluster. Metal covered C_{60} can therefore in a simple picture be modelled with a shell for the cage covered with a new shell originating from the metal atoms. Such a jellium on jellium model has been used by Rubio *et al.* [79] for Na covered C_{60}. Calculations for clusters of Li using a jellium model has however been found to be too crude for a good description of optical response. We have in a number of works [54-56] used a similar classical model and extended it further in a combination with DFT calculations [80]. According to this model C_{60} will have two plasmon energies which will extend to three modes with a metal covered shell. The original modes of C_{60} will shift in energy and also change in intensity.

We have also used the RPA method as outlined above and evaluated the oscillator distribution of C_{60} and metal covered C_{60}. Fig. 6 shows the C_{60} EELS spectrum of Sohmen *et al.* [81] for crystalline C_{60} with the dotted line in (a) and the theoretical oscillator strenghts of C_{60} with the full line in (a) and $Na_{32}C_{60}$ in (b). There is a relative good agreement between the experimental and theoretical spectrum for C_{60} except for a uniform shift of the peaks. We notice how a number of new absorption bands show up in the energy region 1-2 eV for the metal

covered C_{60}. These values of the optical excitations should be compared with the values of the bulk and surface plasmons for Na corresponding to 5.91 and 3.41 eV [82], respectively. The transitions originating from transtions in the metal shell are considerably shifted compared with these more classical values of collective excitations derived from bulk properties.

3.2 Electronic properties of single-wall, nanowire and single-wall filled nanotube

One of the most exciting discoveries in fullerene related research during the last years has been the developments of methods for production of nanotubes of unique electronic properties and the filling of those with different elements. We have for quite some time analyzed the optical properties of multiwall nanotubes, carbon onions [54-56] using the model based classical electromagnetic theory. We have recently used the method outlined above [50] which is able to anlayze the electronic structure of such species as multi-wall nanotubes, nanowires and filled nanotubes. The method is able to perform calculations of systems containing up to thirty thousand of electrons with a jellium background potential. Fig. 7 gives a schemtic picture of the radial charge density and potential for a single-wall nanotube and a Na nanowire. Calculations for such systems with the method given above have given electronic wavefunctions and eigenvalues. We have here chosen to represent the results in terms of Density of States (DOS) diagrams as given in Fig. 8 with the singel nanotube in (a) and the filled nanotube in (b). The most interesting results are the quantization of the DOS in radial and axial direction resulting in DOS curves which are characteristic for mesoscopic systems as quantum wires and quantum dots [83].

4 CONCLUSIONS

In conclusion, the optical properties of C_{60} and metal covered C_{60} has been investigated using a simplified RPA approach. These results are compared with a classical treatment of the collective effects of a spherically averaged radial electronic charge distribution with different number of electrons involved. Some preliminary results are also presented to obtain results for an infinte long single-wall nanotube which is even filled with a nanowire. These new type of model systems opens the direction towards mesoscopic physics and modern technology.

ACKNOWLEDGEMENT

Financual support from, NFR, The Swedish Natural Science Research Council (contract F–FU 2560–128) is gratefully acknowledged.

REFERENCES

1. "Clusters of Atoms and Molecules I and II", Springer-Verlag Berlin Heidelberg 1994 Eds. H. Haberland
2. "ISSPICIConferences 1 to 7" , ISSPIC 1,J. Phys. **38**, (1977), ISSPIC 2, Surf. Sci. **106**, (1981),ISSPIC 3, **156**,(1985), ISSPIC 4, Z. Phys. D **12**, (1989), ISSPIC 5, Z. Phys. D **19/20**, (1991), ISSPIC 6, Z. Phys. D **26/26S**, (1993), ISSPIC 7, Surface Review and Letters **3**, (1996), ISSPIC 8, Z. Phys. D xxx, (1989),
3. W. A. deHeer, Rev. Mod. Phys. , **65**, 611 (1993).
4. M. Brack, Rev. Mod. Phys. , 65, 677 (1993).
5. O. Echt, K. Sattler, and E. Recknagel, Phys. Rev. Lett. 47, 1121 (1981).

6. W. D. Knight, K. Clemenger, W. A. deHeer, W. A. Saunders, M. Y. Chou, and M. L. Cohen, Phys. Rev. Lett. , 52, 2141 (1984).
7. W. Ekardt, Phys. Rev. , 29, 1558 (1984).
8. W. A. deHeer, *et al.*,Solid State Physics, 65, 611 (1993).
9. J. Pedersen, S. Bjornholm, J. Borggreen, K. Hansen, T. P. Martin and H. D. Rsmussen, Nature, **353**, 733 (1991).
10. T. P. Martin, S. Bjornholm, J. Borggreen, C. Brechignac, Ph. Casuzac, K. Hansen and J. Pedersen, Chem. Phys. Lett. , **186**, 53 (1991).
11. T. P. Martin,T. Bergmann, H. Gohlich and T. Lange, Chem. Phys. Lett. , **172**, 209 (1991).
12. "Engineering a Small World", Special section in Science, **254**, 1991)
13. H. Rohrer, Jpn. J. Appl. Phys.,**32**, 1335 (1993).
14. H.W. Kroto, J.R. Heath, S.C. O'Brien, R.F. Curl and R.E. Smalley, Nature, **318**, 162 (1985).
15. W. Krätschmer, K. Fostiropoulos, D.R. Huffman, Chem. Phys. Lett. , **170**, 167 (1990).
16. W. Krätschmer, L.D. Lamb, K. Fostiropoulos, D.R. Huffman, Nature , **347**, 354 (1990).
17. " C_{60} : Buckminsterfullerene, The celestial Sphere that Fell to Earth", Angew. Chem. **31**,111 (1992)
18. "Special Issue on Fullerenes" Carbon, **30**, 1139-1277 (1992) Ed. H. Kroto, Pergamon Press, New York 1992.
19. D.R. Huffman and W. Krätschmer, Mater. Res. Soc. Symp.. **206**, 601 (1991).
20. D.R. Huffman, Physics Today, Nov91, 22 (1991).
21. D.R. Huffman, Adv. Phys. **26**, 129 (1977).
22. "Physics and Chemistry of Fullerene-based Solids" J. Phys. Chem. Solids. **53**, 1992) Eds. J. E. Fischer and D. E. Cox. Pergamon Press New York 1992.
23. Solid State Physics, **48**, 226 (1994) Eds. H. Ehrenreich and F. Spaepen, Academic Press, Boston 1994.
24. "The Chemical Physics of Fullerenes 10 (and 5) Years Later", Natos. ASI Series E: Applied Sciences - Vol. 316 Kluwer Acad. Publ. Ed. W. Andreoni.
25. M. S. Dresselahaus, G. Dresselhaus and P. C. Eklund "Science of Fullerenes and Carbon Nanotubes", Academic Press San Diego 1996.
26. S. Larsson, A. Volosov and A. Rosén Chem. Phys. Lett. **137**, 501 (1987).
27. Z. C. Wu, D. A. Jelski and T. F. George, Chem. Phys. Lett. **137**, 291 (1987).
28. A. Rosén, E. Westin and D. Östling, SPIE Proceedings **2284**, 99 (1994).
29. S.C. O'Brien, J. R. Heath, R.F. Curl and R.E. Smalley, J. Chem. Phys., **88**, 220 (1988).
30. D.S. Bethune, C.H. Kiang, M.S. de Vries, G. Gorman, R. Savoy, J. Vazquez and R. Beyers, Nature, **363**, 605 (1993).
31. S. Ijima, Nature, **354**, 56 (1991).
32. S. Ijima and T. Ichihashi, Nature, **363**, 603 (1993).
33. T. W. Ebbesen, Physics Today, **June 96**, 26 (1996).
34. D. Ugarte, Nature, **359**, 707 (1992).
35. J. Baggott, "Perfect Symmetry: The Accidential Discovery of Buckminsterfullerene", Oxford University Press, Oxford New York 1994.
36. T. P. Martin, N. Malinowski, U. Zimmermann, U. Näher, H. Schaber, J. Chem. Phys., **99**, 4210 (1993).
37. U. Zimmermann, A. Burkhardt, N. Malinowski,U. Näher and T. P. Martin, J. Chem. Phys., **101**, 2244 (1994).
38. U. Zimmermann, N. Malinowski,U. Näher, S. Frank, and T. P. Martin, Phys. Rev. Lett., **72**, 3542 (1994).
39. U. Zimmermann, N. Malinowski, A. Burkhardt, and T. P. Martin, Carbon, , **33**, 995 (1995).
40. M. Springborg, S. Satpathy, N. Malinowski, U. Zimmermann and T. P. Martin, Phys. Rev. Lett., **77**, 1127 (1996).
41. F. Tast, N. Malinowski, S. Frank, M. Heinebrodt, I.M.L. Billas, and T. P. Martin, Z. Phys. D., In press
42. S. Frank, N. Malinowski, F. Tast, M. Heinebrodt, I.M.L. Billas, and T. P. Martin, Z. Phys. D., In press
43. P. M. Ajayan et al , Chem. Phys. Lett., **215**, 509 (1993).
44. P. M. Ajayan and S. Iijima, Nature, **361**, 333 (1993).

45. P. M. Ajayan et al, Nature, 362, 522 (1993).
46. D. S. Bethune et al Nature , 366, 123 (1993).
47. S. Seraphin et al , Nature, 362, 503 (1993).
48. A. Thess et al, Scienc, 273, 483 (1996).
49. T. W. Ebbesen, Nature, 382, 5 (1996).
50. D. Östling, D. Tomanek and A. Rosén Phys. Rev. B. To be published
51. G. Mukhopadhyay and S. Lundqvist, Nuovo Cim., 27B, 1 (1975).
52. G. Mukhopadhyay and S. Lundqvist, J. Phys., B12, 1297 (1979).
53. S. Lundqvist and G. Mukhopadhyay, Physica Scripta, 21, 503 (1980).
54. D. Östling, P. Apell and A. Rosén Europhys. Lett. 21, 539 (1993).
55. D. Östling, P. Apell and A. Rosén Z. Phys. D26, S282 (1993).
56. D. Östling, P. Apell and A. Rosén Electro Chemical Society Proc 94-24, 254 (1994).
57. M. Braga, S. Larsson A. Rosén and A. Volosov, Astron. Astrophys. 245, 232 (1991).
58. G.F. Bertsch, A. Bulgac, D. Tománek and Y. Wang, Phys. Rev. Lett., 67, 2690 (1991).
59. D. Östling and A. Rosén, Chem. Phys. Lett. 256, 109 (1996).
60. E. Westin and A. Rosén, Int. J. Mod. Phys., B6, 3893 (1992).
61. E. Westin and A. Rosén, Appl. Phys. A 60, 49 (1995)5
62. A. Rosén and E. Westi, Surface Review and Letters,3, 729 (1996).
63. "The Electronic Structure of Atoms and Molecules", Addison-Wesely Publ. Comp.Reading Massachusetts 1972.
64. B. Wästberg and A. Rosén, Physica Scripta, 44, 276 (1991).
65. P. Hohenberg and W. Kohn, Phys. Rev., B136, 864 (1964).
66. W. Kohn and L.J. Sham, Phys. Rev., A140, 1133 (1965).
67. L. Hedin and B.I. Lundqvist, J. Phys., C4, 2064 (1971).
68. P. M. Boerrigter and G. Te Velde and E. J. Baerends, Int. J. Quant. Chem., 33,87 (1988).
69. A. Rosén, D.E. Ellis, H. Adachi and F.W. Averill, Chem. Phys., 65, 3629 (1976).
70. B. Delley and D.E. Ellis, J. Chem. Phys., 76, 1949 (1982).
71. J. D. Jackson, "Classical Electrodynamics", Second Edition, John Wiley and Sons, New York, 1975.
72. S. Salomonson and P. Öster, Phys. Rev. A, 40, 5559 (1989).
73. D. J. Rowe, "Nuclear collective motion", Meuthen, London 1970.
74. C. Yannouleas and R. A. Broglia, Phys. Rev. A, 41, 5793 (1991).
75. M. Madjet, C. Guet and W. R. Johnson, Phys. Rev. A, 51, 1327 (1995).
76. K. Hedberg, L. Hedberg, D.S. Bethune, C.A. Brown, H.C. Dorn, R.D. Johnson and M. de Vries, Science, 254, 410 (1991).
77. J. Kohanoff, W. Andreoni and M. Parinello, Chem. Phys. Lett. 198, 472 (1992).
78. U. Zimmermann, A. Burkhardt, N. Malinowski, U. Nand T. P. Martin, J. Chem. Phys., 101, 22441 (1994).
79. A. Rubio, J. A. Alonso, J. M. Lopez and M. J. Stott, Phys. Rev. B., 49, 17397 (1994).
80. D. Östling and A. Rosén, Electro Chemical Society Proc 95-10, 1232 (1995).
81. E. Sohmen, J. Fink and W. Krätschmer, Z. Phys. B, 86, 87 (1992).
82. N. W. Ashcroft and N. D. Mermin, "Solid State Physics", Saunders College Publishing, 1976.
83. J. I. Pascual et al, Science 267, 1793 (1995).

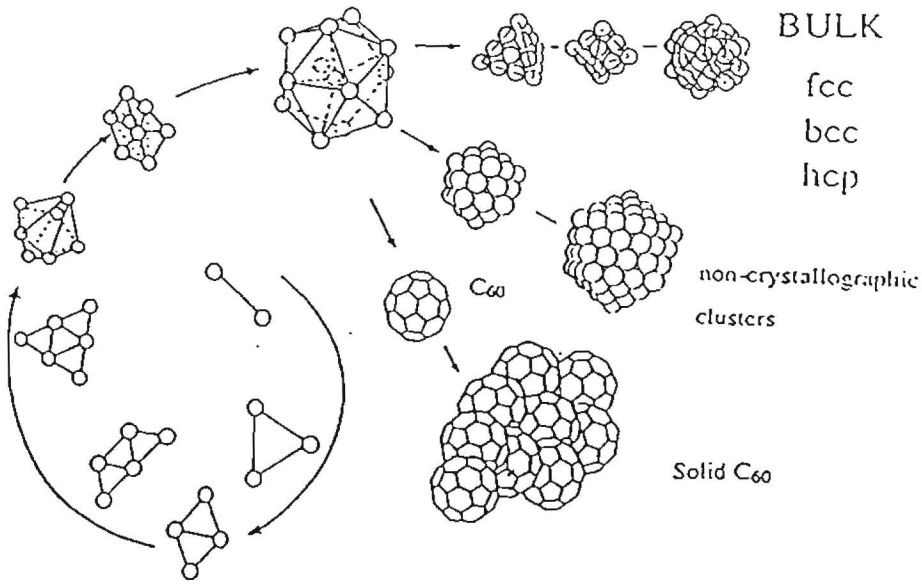

Figure 1: Schematic overview of the growth of clusters when atoms are added to the smaller units in the formation of species with bulk properties as exemplified with fcc, bcc and hcp crystal structure. In addition very unique structures have been discovered as noncrystallographic clusters and the fullereens. The most wellknown fullerene C_{60} has also been used in the growing of crystals.

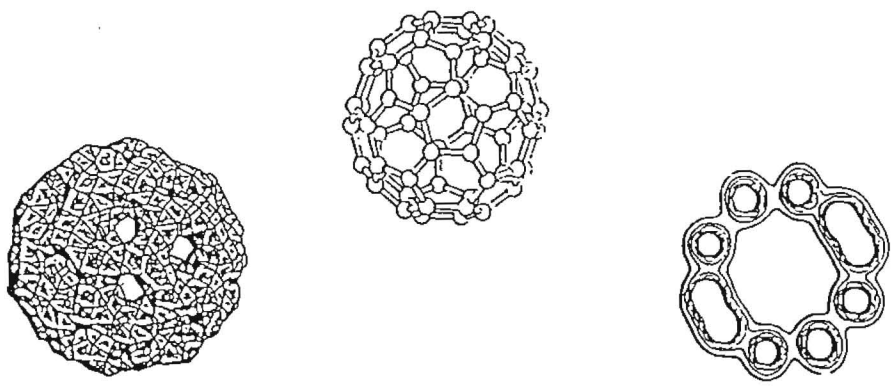

Figure 2: A schematic overview of C_{60} represented by a stick model, 3D and 2D contour plots of the electron density. In the 3D plot to the left the single contour has been chosen to show how the electrons are distributed in the bonds. The 2D contour plot shows the electron density in a plane that includes the center of the molecule. We clearly see that there is a large void, which means that C_{60} consitutes a spherical shell.

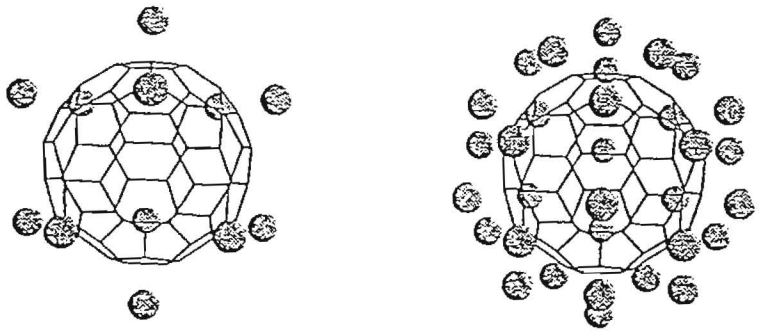

Figure 3: A schematic overview of metal coverd C_{60} with 12 and 32 metal atoms located above the pentagons and hexagons.

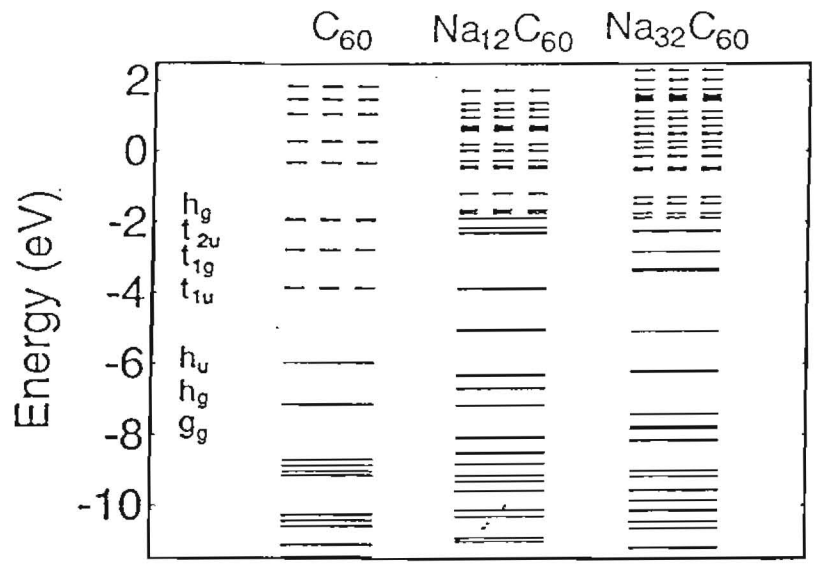

Figure 4: Energy level diagram of C_{60} and Na covered C_{60} with 12 and 32 atoms

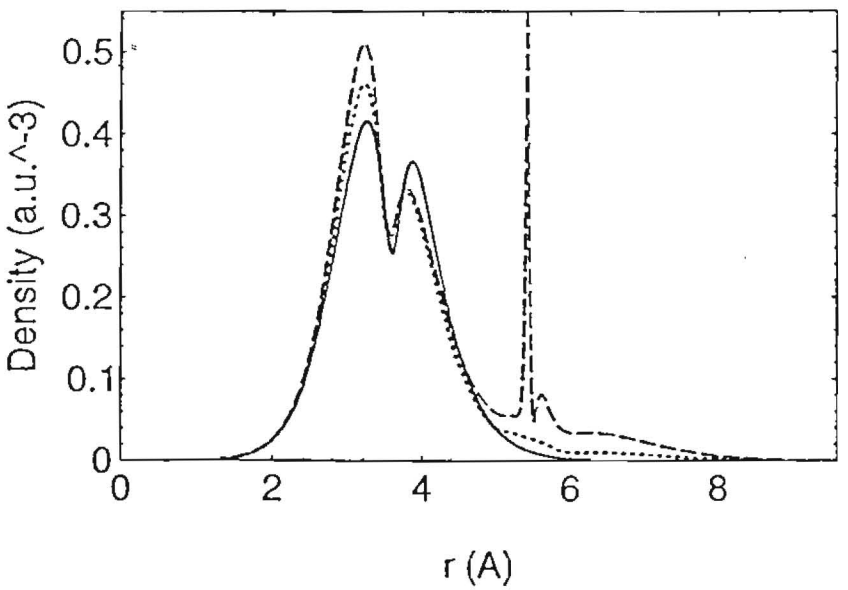

Figure 5: Spherical radial average charge densities of the 60 π electrons of C_{60} full line and the first 72 electrons of $Na_{12}C_{60}$and 92 electrons of $Na_{32}C_{60}$. The position of the Na atoms have been chosen as given in the text

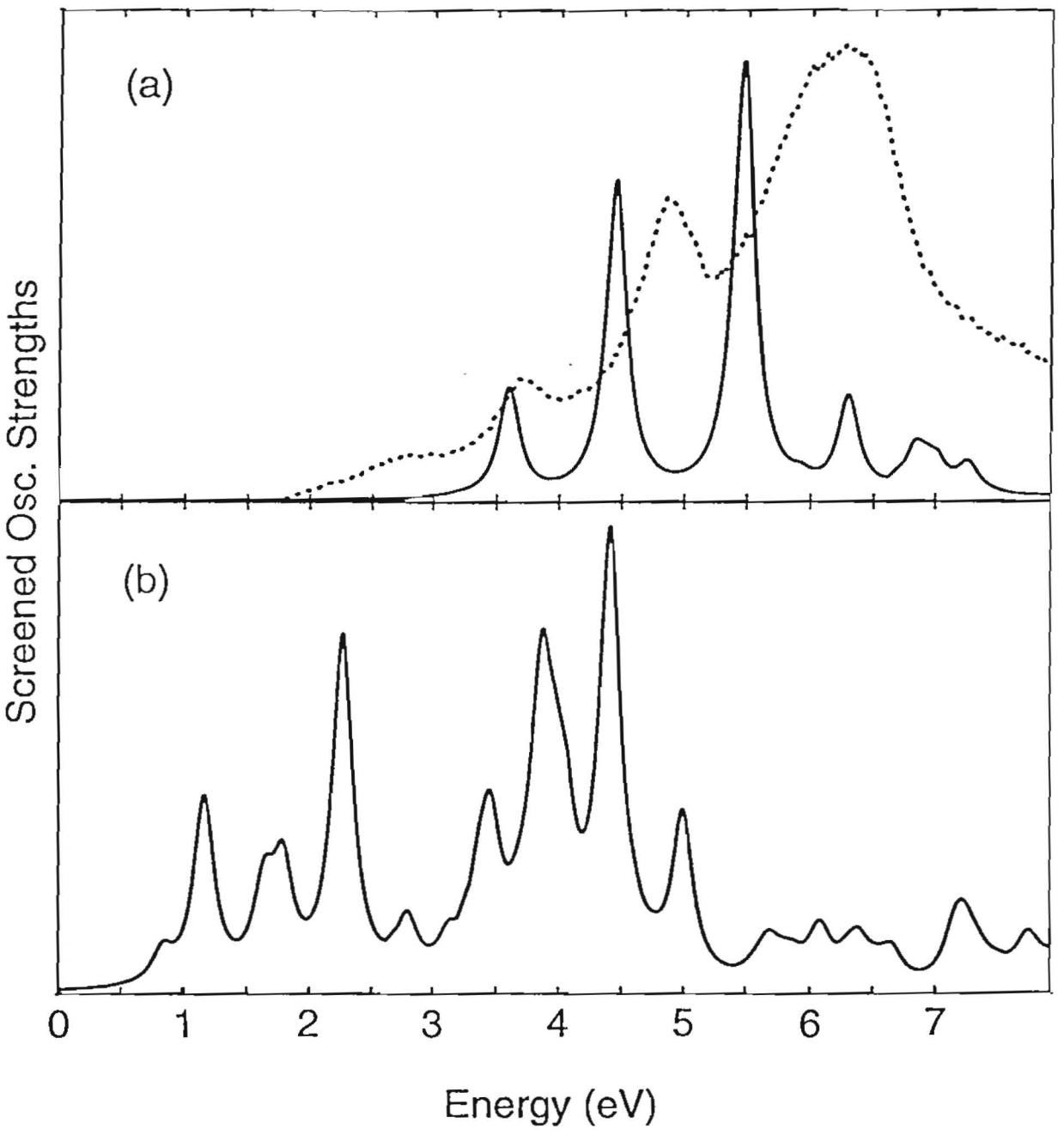

Figure 6: In (a) the experimental results of Sohmen *et al.* [81] for crystalline C_{60}, dotted line, and the theoretical oscillator strengths, full line, and in (b) the theoretical oscillator strengths of $Na_{32}C_{60}$. All the theoretical strengths are evaluated using the RPA approach

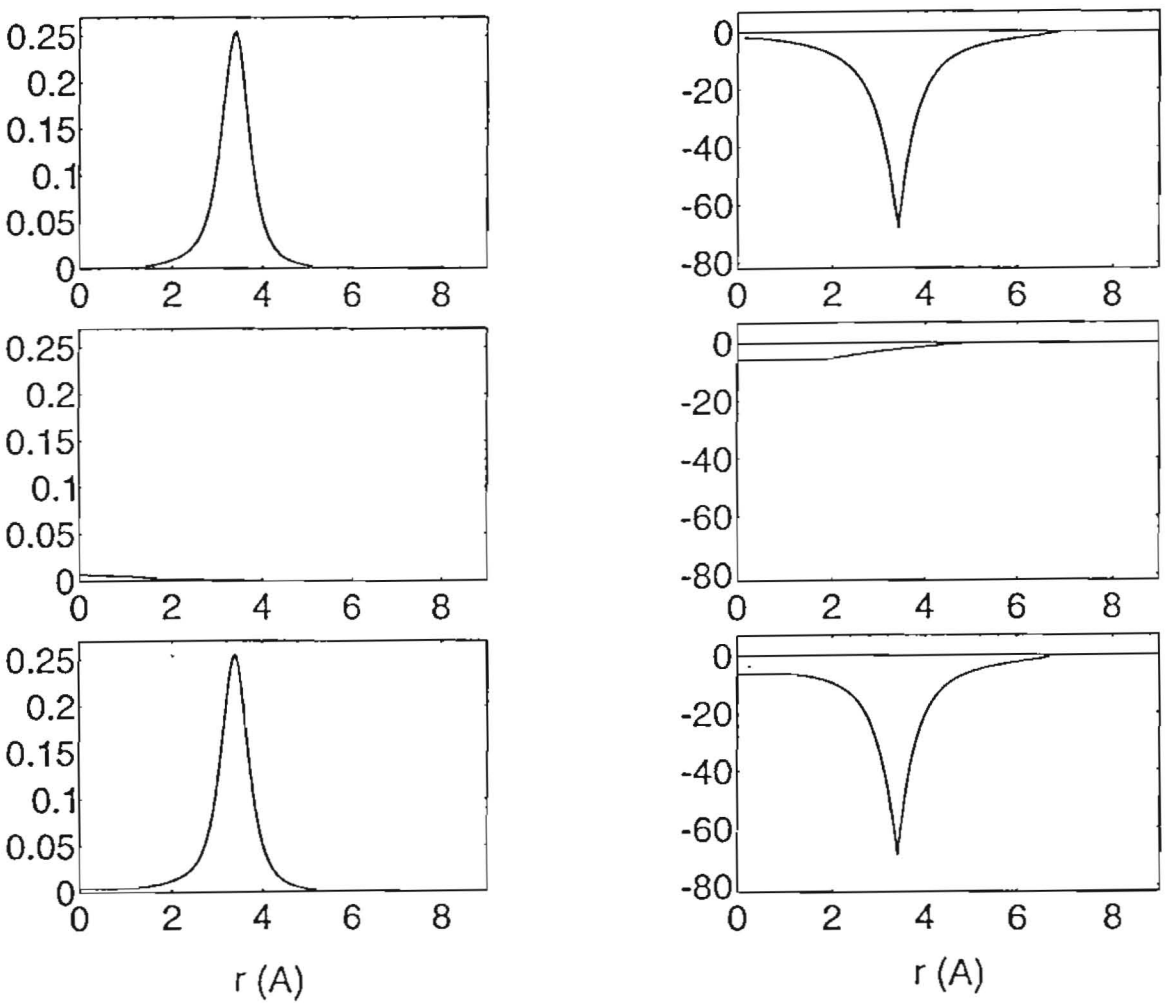

Figure 7: Results from self-consistent radial density, left part of the figure, and effective potential, right part of the figure. The upper part of the figure shows the result of a single-wall nanotube with radius R = 3.4$\mathring{A}$, the middle part the result of a solid nanowire with R = 2.4 $\mathring{A}$ and the lower part the result of a single wall nanotube filled with the nanowire

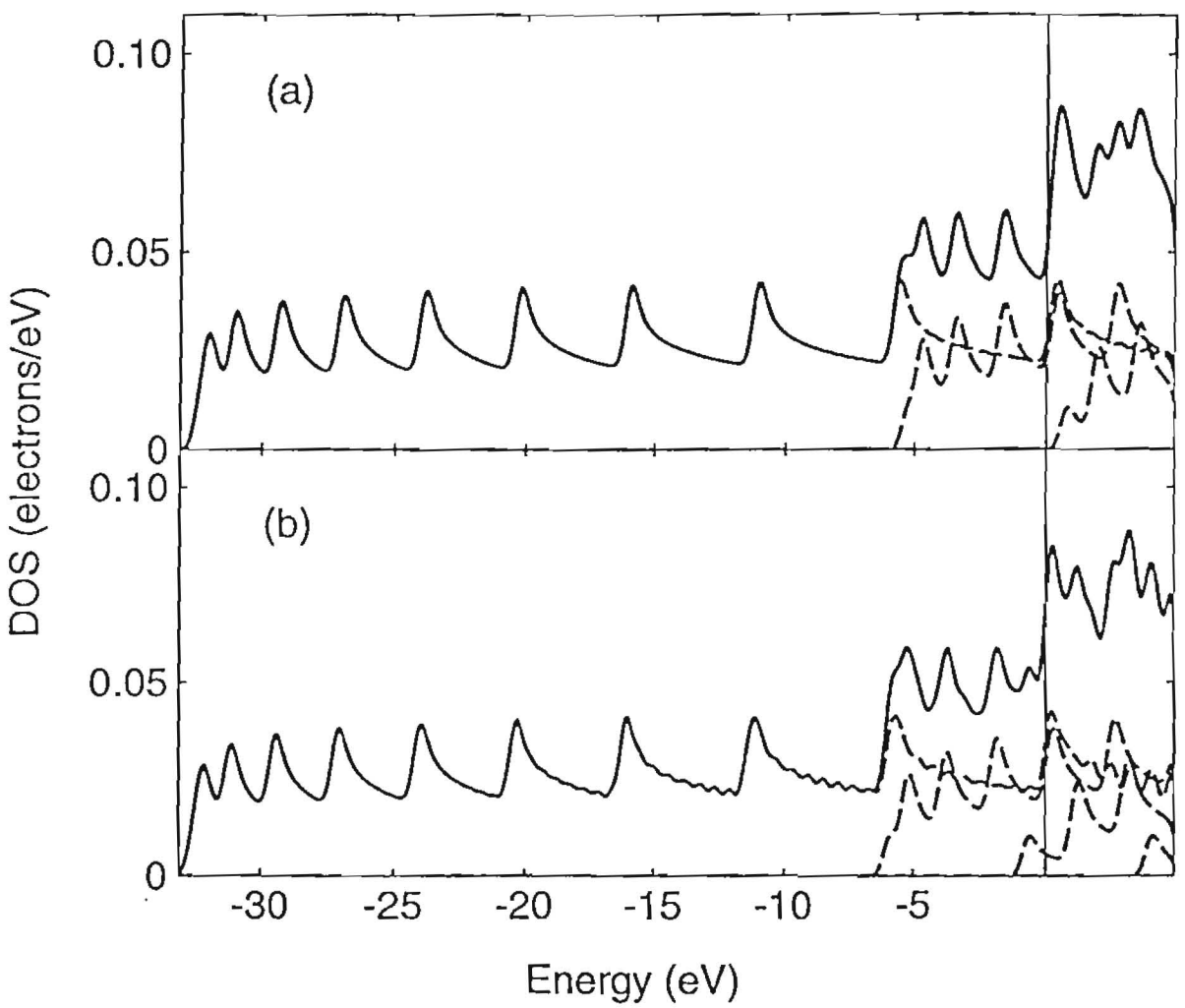

Figure 8: The electronic density of states (DOS) of single-wall nanotube (a) and a single-wall nanotube filled with a nanowire (b).